J Solid State Electrochem (2011) 15:649–662
DOI 10.1007/s10008-010-1264-9

REVIEW

# Separator technologies for lithium-ion batteries

**Xiaosong Huang**

Received: 11 October 2010 / Revised: 20 November 2010 / Accepted: 28 November 2010 / Published online: 30 December 2010


**Abstract** Although separators do not participate in the electrochemical reactions in a lithium-ion (Li-ion) battery, they perform the critical functions of physically separating the positive and negative electrodes while permitting the free flow of lithium ions through the liquid electrolyte that fill in their open porous structure. Separators for liquid electrolyte Li-ion batteries can be classified into porous polymeric membranes, nonwoven mats, and composite separators. Porous membranes are most commonly used due to their relatively low processing cost and good mechanical properties. Although not widely used in Li-ion batteries, nonwoven mats have the potential for low cost and thermally stable separators. Recent composite separators have attracted much attention, however, as they offer excellent thermal stability and wettability by the nonaqueous electrolyte. The present paper (1) presents an overview of separator characterization techniques, (2) reviews existing technologies for producing different types of separators, and (3) discusses directions for future investigation. Research into separator fabrication techniques and chemical modifications, coupled with the numerical modeling, should lead to further improvements in the performance and abuse tolerance as well as cost reduction of Li-ion batteries.

**Keywords** Lithium-ion battery · Separator · Porous membrane · Battery abuse tolerance · Thermal runaway

## Introduction

Secondary lithium-ion (Li-ion) batteries provide an attractive landscape for energy storage systems due to their high specific energy (about 150 Wh/kg), high-energy density (about 400 Wh/L), long lifetime cycle (>1,000 cycles), low self-discharge rate (2–8%/month), and high-operational voltage (2.5–4.2 V) [1]. They have been widely used in consumer electronics, such as portable computers, camcorders, and cell phones [2]. Recently, their applications have been expanding into aerospace technology, electric vehicles (EV), and hybrid-electric vehicles (HEV) [2].

*Lithium-ion battery design* Typically produced in either spiral wound or prismatic design, the four fundamental components of a Li-ion battery are the negative electrode (anode), the positive electrode (cathode), the electrolyte, and the separator, as shown schematically in Fig. 1. The first three components participate in the electrochemical reactions in a battery cell, while the separator is an inactive component.

Most of Li-ion batteries use carbon as the active anode material, although silicon, lithium titanate, tin dioxide, and some intermetallics have also been intensely researched [3–6]. This active material is adhered to a copper current collector with a binder, typically poly(vinylidene fluoride) (PVDF), and a high-surface-area carbon (e.g., acetylene black) is used in the electrode formulation in order to provide an electron flow path to the current collector.

Lithiated transition metal oxides have been widely used as the active materials for cathodes. Similarly to the negative electrode, the active material particles are adhered to an aluminum current collector with a binder. A high-surface-area carbon is also incorporated to provide a conductive path for the electrons to reach the active material particles.

The last active component in a Li-ion battery is the electrolyte. An electrolyte composition requires good chemical, thermal, and electrochemical stability, as well as high-ionic conductivity. Despite its known disadvantages (problematic thermal stability and susceptibility to hydrolysis with the formation of hydrofluoric acid), lithium hexafluorophosphate ($LiPF_6$) dissolved in a mixture of organic solvents represents

X. Huang (✉)
Chemical Sciences and Materials Systems Lab,
General Motors Global R&D,
30500 Mound Rd.,
Warren, MI 48090, USA
e-mail: xiaosong.huang@gm.com

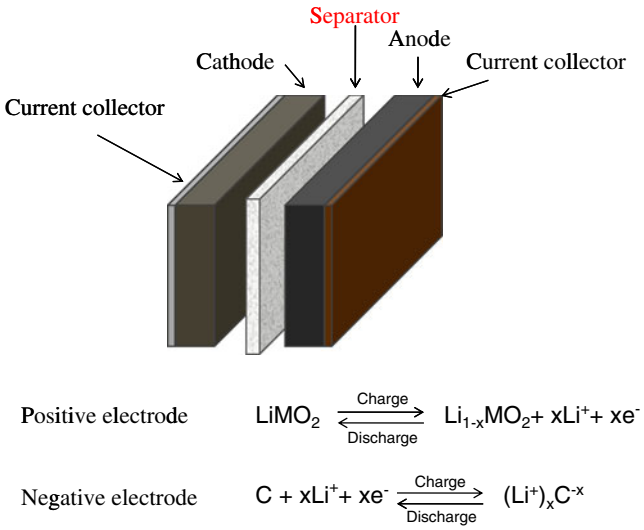


**Fig. 1** Schematic of a liquid electrolyte Li-ion cell

the most widely used liquid electrolyte due to its relatively low-cost, high-ionic conductivity, and the ability of passivating the aluminum current collector for the positive electrode. Generally, the organic solvents used for dissolving $LiPF_6$ are carbonates, such as ethylene carbonate (EC), propylene carbonate (PC), dimethyl carbonate (DMC), ethyl methyl carbonate (EMC), and diethyl carbonate (DEC). During the battery operation, lithium ions ($Li^+$) are shuttled between the anode and cathode via the electrolyte—from the anode to the cathode during discharging and in the reverse direction during the charging of the battery.

The only inactive fundamental component of a Li-ion battery cell is the separator, necessarily sandwiched between the anode and cathode. It plays two main roles during the successful operation of a cell: (1) resting between the anode and cathode to prevent internal short circuiting and (2) providing a path for ionic conduction in the liquid electrolyte throughout the interconnected porous structure. Separators for liquid electrolyte batteries are currently engineered as porous membranes, nonwoven mats, or multilayers consisting of porous membranes and/or nonwoven mats [7, 8]. Table 1 lists the major separator manufacturers, showing that most of the commercial separators are made of porous polyolefin membranes.

*Separator requirements* An ideal separator should have an infinite electronic but a zero ionic resistance. In practice, the electrical resistivity of the polymers used for separators is in the order of $10^{12}$–$10^{14}$ Ω cm, i.e., they are electrical insulators. In the meantime, a low internal ionic resistance is especially important for HEV/EV applications where a battery needs to be able to offer high power. However, the existence of the separator always increases the ionic resistance of the inter-electrode medium (consisting of the separator and the liquid electrolyte) because (1) the finite porosity of a separator implies a restricted contact area between the electrolyte and the electrodes, and (2) the tortuosity of the open porous structure results in a longer mean path for the ionic current compared to when the liquid electrolyte is used alone. Generally, a thin membrane with a high porosity and a large mean pore size can minimize the ionic resistance, enabling high-specific battery power. However, too great of a porosity and a small membrane thickness can reduce the mechanical strength of the membrane and increase the risk of inner battery electrical shorting. In practice, most separators for liquid electrolyte batteries in use today are 20 to 30 μm thick, have submicron-sized pores, and possess porosity ranging from 40% to 70%.

In addition, the separator should be mechanically strong, with no skew or yield, to keep the anode and cathode from contacting each other during the whole battery lifetime. Separators also must possess dimensional stability at elevated temperatures, especially for applications in high-power batteries. Fully charged batteries have highly oxidizing and reducing environments at electrode–electrolyte interfaces, the stability of a separator in these environments is therefore critical. The specifications for a liquid electrolyte battery separator provided by the US Advanced Battery Consortium (USABC) are listed in Table 2.

*Significance of separator development* Despite their advantages over the alternative battery technologies, the application of large-capacity Li-ion batteries is hindered mainly due to the cost, the abuse tolerance concerns, and the loss of performance, especially at extreme operating temperatures. The further development in separator technologies will help facilitate the expansion of the application of Li-ion batteries.

**Table 1** Major separator manufacturers

| Manufacturer | Material | Separator design |
|---|---|---|
| Asahi Kasei chemicals | Polyolefin and ceramic-filled polyolefin | Biaxially orientated |
| Celgard LLC | PE, PP, and PP/PE/PP | Uniaxially orientated |
| Entek membranes | Ceramic-filled UHMWPE | Biaxially orientated |
| ExxonMobil/Tonen | PE and PE/PP mixtures | Biaxially orientated |
| SK energy | PE | Biaxially orientated |
| Ube industries | PP/PE/PP | Uniaxially orientated |

*PE* polyethylene, *PP* polypropylene, *PET* poly(ethylene terephthalate), *UHMEPE* ultrahigh molecular weight polyethylene

**Table 2** USABC requirements for Li-ion battery separators

| Parameter | Goal | Test method |
|---|---|---|
| Sales price ($/m$^2$) | ≤1.00 | |
| Thickness (μm) | ≤25 | ASTM D5947-96, ASTM D2103 |
| MacMullin number | ≤11 | N/A |
| Gurley (s/10 cm$^3$) | <35 | ASTM D726 |
| Wettability | Complete wet-out in typical battery electrolyte | N/A |
| Chemical stability | Stable in battery for 10 years | N/A |
| Pore size (μm) | <1 | ASTM E128-99 |
| Puncture strength | >300 g/25.4 μm | ASTM F1306-90 |
| | | ASTM D3763 |
| Thermal stability | <5% shrinkage at 200 °C | ASTM D1204 |
| Purity | <50 ppm $H_2O$ | N/A |
| Tensile strength | <2% offset at 1,000 psi | ASTM D882-00 |
| Skew (mm/m) | <2 | N/A |
| Pin removal | Easy removal from all major brands of winding machines | N/A |
| Melt integrity | ≥200 °C | Thermal-mechanical analysis |

One of the major concerns for Li-ion batteries centers on the thermal events triggered by hard internal shorts. The cause can be traced back to the manufacturing process when defects (metal fines) are introduced into the inter-electrode space. Separators are considered to be a crucial battery component for avoiding thermal runaway conditions. Although the separators with thermal shut-down ability have been commercially available since the 1990s, they have been ineffective for preventing the hard internal shorts that originate from the manufacturing defects. Two (not necessarily incompatible) technological solutions for mitigating the internal shorting have therefore been proposed during the past several years: (1) separators exhibiting a high melting point, a low high-temperature shrinkage, and improved mechanical properties (in particular, puncture resistance) and (2) ceramic-enhanced separators, either containing ceramic layers on their surfaces or having ceramic powders dispersed in the polymeric material, where the major role of the ceramic is to prevent the collapse of the inter-electrode space and thus avoid an internal short in the event of thermal runaway conditions.

In addition, separator accounts for a large portion of the cost of a battery cell, which can exceed 20% for a high-power battery. The USABC cost target for a separator is $1/m$^2$ as indicated in Table 2. Research into separator fabrication techniques to develop low-cost separators is therefore critical to reduce the overall cost of the battery system.

The present paper presents an overview of separator characterization techniques, reviews existing technologies for producing different types of separators, touches upon the numerical modeling, and discusses directions for future investigation.

## Separator characterization

*Electrolyte resistance derating factor* The incorporation of a porous separator increases the ionic resistance of the inter-electrode medium. The so-called MacMullin number ($N_M$), shown below in Eq. 1, is a relative value used to describe the increased resistance of the inter-electrode medium, caused by the presence of a separator, relative to the resistance of the liquid electrolyte by itself, assuming equivalent dimensions between the electrodes for each [9–11]:

$$N_M = \frac{R_s}{R_0} \tag{1}$$

where $R_s$ is the resistance of the inter-electrode medium once a separator is sandwiched between the electrodes, and $R_0$ is the resistance of the liquid electrolyte.

Figure 2 is a simplified alternating current impedance spectrum (Nyquist plot), commonly used to determine the resistance. In Fig. 2, the semicircle (or overlapped semi-circles) is due to different physical electrochemical processes and the observed Warburg line in some cases can be related to the diffusion of $Li^+$. Ideally, $N_M$ should be close to one, while the typical values of the $N_M$ for Li-ion battery separators range from 5 to 15.

Besides the development of solid electrolyte interphase (SEI) on the electrode particle surface, the compatibility between the separator and the electrodes can also change the cell resistance. As indicated in Fig. 2, the total interfacial resistance ($R_i$ or $R_{SEI}$) can be estimated by subtracting the bulk resistance ($R_b$) in the complex impedance spectrum. Jeong and Kim [12] observed that after increasing the thickness of a porous gellable poly

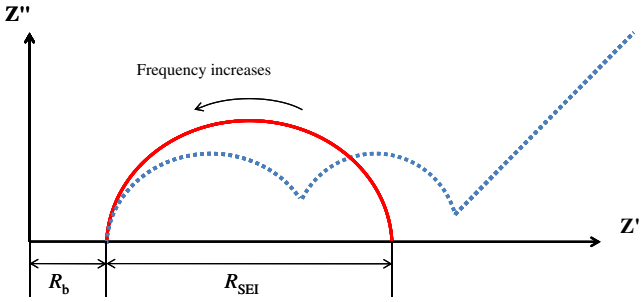


**Fig. 2** Schematic of a simplified AC impedance spectrum

(acrylonitrile-*methyl* methacrylate), layered on a polyolefin separator, from 4 to 14 μm, the $R_i$ dropped from 50.4 to 40.1 Ω cm$^2$. This observation in reduction was contributed to better interfacial adhesion.

*Porosity, mean pore size, tortuosity, and permeability* The morphology of a separator affects not only the battery performance and abuse tolerance but also the efficiency of assembling and handling of a battery through its mechanical and physical properties.

Porosity can be determined by a simple liquid absorption test according to ASTM D2873 [13], from Eq. 2,

$$P = \frac{w_T - w_s}{\rho_l \cdot V_s} \tag{2}$$

where $w_s$ is the weight of the dry separator sample, $w_T$ is the total weight of the separator once the liquid is fully absorbed, $\rho_l$ is the density of the liquid, and $V_s$ is the apparent volume of the separator sample.

Separators should have small mean pore sizes and uniform pore size distributions. Small mean pore sizes are preferred as they can effectively prevent shorts caused by dendrite growth or the migration of the active material particles between battery electrodes. Uniform pore size distributions can avoid the nonuniform current densities across the electrode-separator interfaces. A nonuniform current accelerates the formation of Li dendrites in a cell. Pore dimension and pore size distribution can be estimated from porosimetry techniques based on the Laplace equation [14] as shown below in Eq. 3:

$$d = -\frac{4\gamma \cos\theta}{\Delta P} \tag{3}$$

where $d$ is the pore diameter, $\Delta P$ is the pressure difference across the pore, $\gamma$ is the surface tension of the liquid, and $\theta$ is the contact angle. Based on this equation, different types of porometers have been developed to characterize complex porous structures as discussed in the review paper by Jena and Gupta [15]. For a more qualitative approach, cross section and surface pore morphologies can be examined simply from scanning electron microscopy images.

The tortuosity factor indicates the ratio of the mean actual path in comparison with the direct distance. Tortuosity τ [3, 16] can be estimated from Eq. 4 as shown below:

$$\tau = \sqrt{\varepsilon \frac{R_s}{R_0}} \tag{4}$$

where $\varepsilon$ is the porosity ratio. A high tortuosity hinders the growth of Li dendrites but increases the ionic resistance of the inter-electrode medium.

The permeability is typically characterized using the Gurley number according to ASTM D726. It measures the time for a given amount of gas to flow through the membrane at a constant pressure. Clearly, the Gurley number will depend on the porosity, the fraction of open pores, and the tortuosity of a separator. The permeability can also be evaluated from the permeability coefficient B according to Darcy's law, from Eq. 5 shown below. Here, $l$ is the sample thickness, $\mu$ is the fluid viscosity, $v$ is the fluid velocity, and $\Delta P$ is the pressure drop across the separator [17].

$$B = \frac{l\mu v}{\Delta P} \tag{5}$$

*Wettability* The separator should quickly absorb and retain the electrolyte during operation. Poor wettability limits the performance of a cell by increasing the internal ionic resistance. Good wettability shortens the electrolyte filling time during the cell assembly and extends the battery's life cycle under normal operating conditions. There is no standard method for the wettability test although measuring the contact angle between the liquid electrolyte and the separator is a simple indicator. An alternative method to determine wettability is by hanging a separator vertically in a liquid electrolyte and calculating the wicking (capillary rise) rate or height.

*Thermal behavior* Most commercial separators provide thermal shutdown (fuse) capability at various temperatures. Upon reaching a certain temperature, the separator can flow and fuse into a film by pore collapsing, thus, minimizing the ionic conduction between the electrodes and protecting batteries from overheating or electrical shorting. Thermal shutdown must start before the occurrence of the uncontrollable thermal runaway and can be evaluated by measuring the resistance as the temperature increases. Venugopal et al. [13] tested different membranes, as shown in Fig. 3, where a polypropylene (PP) membrane exhibited shutdown at around 165 °C and the resistance increased approximately by two orders of magnitude; a polyethylene (PE) separator showed shutdown at around 135 °C and the electrical resistance increased by about three orders of magnitude. It was reported that at least a three order of magnitude

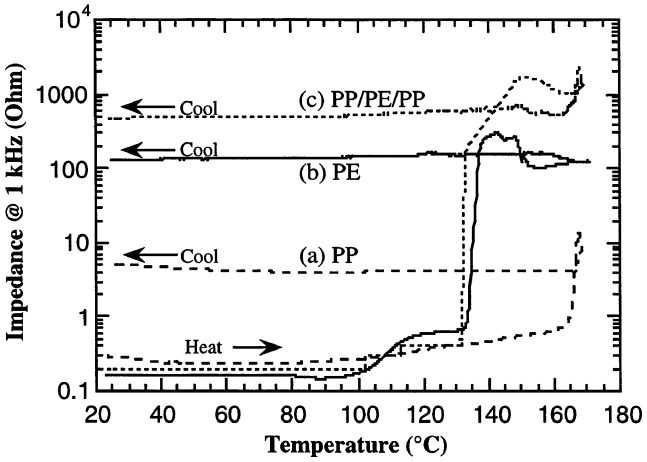


**Fig. 3** Separator thermal shutdown [13]

increase in the electrical resistance was required to effectively shut down the reactions.

A separator must also prevent the electrodes from contacting one another at high temperatures. Therefore, its shrinkage at an elevated temperature needs to be minimized. Thermal-mechanical analysis can be used to characterize the high-temperature shrinkage of a separator. The separator is held under a constant load while simultaneously recording the elongation and temperature change. Porous separators that are either uniaxially or biaxially stretched usually have a large shrinkage in the stretched direction, while ceramic separators can offer high-dimensional stability at elevated temperatures.

*Mechanical properties* A certain mechanical strength is required for separator handling, battery assembly, and abuse tolerance consideration. The most important mechanical properties are the tensile strength and puncture strength. Tensile properties are measured by the conventional stretching process according to ASTM D882. The strength is strongly influenced by the post-extrusion stretching. Porous membranes usually show a high tensile strength in the stretched direction. The puncture strength is the load required for a needle to puncture a separator and can be tested according to ASTM F1306. The USABC puncture strength target is 300 g/25.4 μm, as indicated in Table 2. High puncture strength helps to deter dendrites or particles from penetrating the battery separators.

## Polymeric porous membranes

*Manufacturing processes* The most widely used processes for producing porous polymeric membranes for liquid electrolyte Li-ion batteries are the dry and wet processes. Both processes are conducted through an extruder and employ stretching in one or two directions to impart/increase the porosity and improve the tensile strength. Both processes use low-cost polyolefin materials, and thus the majority of the separator cost is due to manufacturing methodologies.

In the dry process, the melt-extruded polyolefin films are annealed at an elevated temperature immediately below the polymer melting temperature to induce crystallite formation and/or to increase the size and amount of crystallites. The well-aligned crystallites have lamellae arranged in rows, perpendicular to the machine direction. Uniaxial stretching at a low temperature and a subsequent high temperature is followed. The stretching of about 150–250% in the machine direction can be achieved by utilizing nip rolls with different circumferential rates. The porous structure is formed in this step due to the fracturing of the amours phase or tearing apart of the lamellar crystallites. Heat treatment is then followed to fix the pores and relax the residual stress in the membrane. Porous membranes produced through this dry process usually show characteristic slit-like pore structures, as shown in Fig. 4a [7]. It is obvious that nanosized fibrils connect adjacent crystalline regions. The stretching ratio, speed, temperature, and other processing parameters dictate the membrane morphology. US patents 4994335, 4138459, 3801404, and 3843761 have described this process in detail. Generally speaking, a uniaxially stretched membrane exhibits good mechanical properties (>150-MPa tensile strength) but a high thermal shrinkage in the machine direction, while a low tensile strength (<15 MPa) but a negligible thermal shrinkage in the transverse direction. Dry process requires no use of solvents. However, this type of process is only applicable to polymers that can form semicrystalline structures.

In the wet process, plasticizers (or low molecular weight substances, e.g., paraffin oil and mineral oil) are added into the polymer before it is extruded or blown into a thin film at an elevated temperature. The extruded film is then calendared until a desired thickness is achieved. After solidification, the plasticizer is extracted from the film with a volatile solvent (e.g., methylene chloride and trichloroethylene) to leave submicron-sized pores. The porous membrane then passes through a solvent extractor to remove the solvent in it after it leaves the oil extraction tank. The separators fabricated through this wet process are generally stretched biaxially to enlarge the pore size and increase the porosity. Therefore, the pores are more round-like as indicated in Fig. 4b [7]. Tensile strengths in the machine and transverse directions are comparable and can both exceed 100 MPa. Compared with the dry process, this wet process can be applied on a wider range of polymers since there is no requirement on the formation of a semicrystalline structure before stretching. In addition, the application of plasticizers reduces the viscosity, thus,

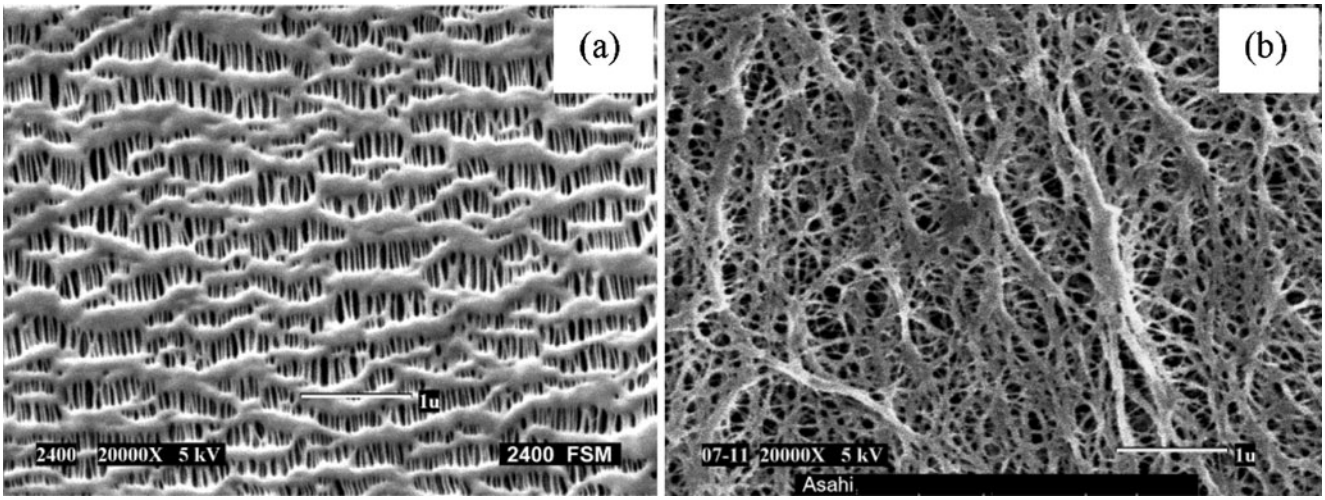


**Fig. 4** Separators fabricated by the dry (**a**) and the wet (**b**) processes [7]

improving the polymer processability. However, the plasticizer extraction in this wet process adds cost to the membrane production. This step needs to be designed to prevent an undesired release of solvent from the system.

Parameters such as dope composition, quenching temperature, stretching rate, and film thickness can all influence the membrane morphology. Kim and Kim [18] investigated the pore size control by generating a phase diagram. Membranes were fabricated with PE/dioctyl phthalate (DOP), PE/isoparaffin, and PE/DOP/isoparaffin, respectively. The average pore size varied from 0.07 to 0.5 μm depending mainly on the temperature gap between the phase separation and PE crystallization. Ma et al. [19] have shown that stretching before plasticizer extraction can produce membranes with a smaller mean pore size and a narrower pore size distribution compared with stretching after the extraction. Fillers can also be used to change the morphology and improve the mechanical and thermal performance of a membrane [20, 21]. Yoneda et al. [20] investigated the phase separation behavior of a three-component system consisting of PE, nanosilica powder, and a solvent (or plasticizer). They reported that the addition of silica resulted in a greater mean pore size.

Besides the dry and wet processes, there are a couple of other techniques that have been studied to produce porous membranes for Li-ion battery applications. Phase inversion is a well-known technique to prepare porous membranes [22–28]. A polymer solution is cast into a thin film and then soaked in a nonsolvent coagulation bath. Since the solvent and nonsolvent are miscible, a rapid diffusion rate of the nonsolvent and solvent causes phase separation to take place, forming a solid-like polymer rich phase and a liquid-like polymer lean phase. In the case when the polymer rich phase is a continuous phase, a porous membrane can be formed when the polymer lean phase is replaced by the nonsolvent after a further solvent/nonsolvent exchange. The parameters that can change the membrane morphology include but are not limited to solvent, nonsolvent, composition of the polymer solution, and coagulation temperature. Zhang et al. [29] used acetonitrile as a solvent and water as a nonsolvent to fabricate a porous membrane of poly (vinylidene fluoride-co-hexafluoropropylene) (PVDF-HFP) by this phase-inversion process. They observed different morphologies on the two sides of the porous membrane as one side of the cast solution film had been in contact with a solid substrate while the other side had been exposed to the nonsolvent. Andrieu and Laurence [30] cast a PVDF solution directly onto a negative electrode and, by immersing the negative electrode in water, a porous separator membrane with a porosity of 75% was formed.

The evaporation-induced phase separation is very similar to the abovementioned phase-inversion process. It takes the advantage of the differential evaporation rates of the solvent and the nonsolvent to form a porous structure. A composition consisting of a polymer, a volatile polymer solvent, and a less volatile nonsolvent can be cast into a thin film. The solvent and the nonsolvent ideally should be completely miscible. With the evaporation of the solvent, the film solidifies and the nonsolvent is homogeneously dispersed in the matrix. The subsequent removal of the nonsolvent yields a porous structure. Similarly, solvent, nonsolvent, polymer concentration, polymer solubility, etc. can all change the membrane morphology. It has also been reported that fine fillers can be added to the polymer solution to maintain the porous structure and provide structural strength to the produced membrane [31–33].

*Polymers for the fabrication of porous separators* Most of the commercially available Li-ion battery separators are made of PE, PP, other polyolefins, or their mixtures, or copolymers through either a dry or wet process. Polyolefin usually provides good mechanical properties and chemical

stability. Most of the polyolefin separators can also provide thermal shutdown capability at various temperatures by closing the pores and turning the membrane into a nonporous film. The thermal shutdown temperature of a PP membrane is around 160 °C, while the thermal shutdown temperature of PE is between 120 and 150 °C, depending upon its morphology. Ultrahigh molecular weight PE (UHMWPE) has good melt integrity and sufficient polymer flow to cause pore collapse, thereby providing better thermal shutdown through the formation of a nonporous film.

Although polyolefin materials can provide thermal shutdown at an appropriate temperature range, the temperature in a cell may continue to increase after the pores are closed. It is possible that the separator would shrink, melt, and finally lead to the shorting of the electrodes. Therefore, to ensure good abuse tolerance, the difference between the shutdown temperature and the melting temperature should be as large as possible. Coextrusion or lamination of PP and PE to produce multilayer membranes has been used for this purpose. PP/PE bilayer separators and PP/PE/PP trilayer separators have been developed [34, 35]. The PE layer transforms into a nonporous film at a temperature lower than the thermal runway temperature, which increases the electrical resistance and provides thermal shutdown. In the meantime, the PP layers still maintain mechanical integrity and keep the electrodes separated.

Instead of lamination, Higuchi et al. [36] patented a battery separator made of a blend of PE and PP. The separator was produced by a dry process. Since PP and PE are not completely miscible, the separator showed porous regions of PE and PP. The separator provided the thermal shutdown ability at a temperature close to the melting point of PE. PP maintained the mechanical integrity of the separator up to its melting temperature.

Ihm et al. [37] made separators using the blends of a high-density polyethylene (HDPE) and an UHMWPE by a wet process. They concluded that the mechanical strength of the membranes increased with the molecular weight of UHMWPE and its content in the blends. The film consisting of 6 wt.% UHMWPE at a draw ratio of 5 showed a tensile strength of about 100 MPa. Although the tensile strength increased with the draw ratio, the puncture strength decreased. The pore size was very uniform and most of the pores arranged in size from 0.10 to 0.12 μm.

Nitto Denko Co. developed a UHMWPE separator having a crosslinked structure. UHMWPE resin blended with a crosslinkable rubber was made into a porous membrane by a wet process [38, 39]. The porous membrane was then crosslinked by air oxidation. The final structure showed high puncture strength and heat rupture resistance.

Johnson and Wilkes [40] prepared porous membranes made of an isotactic poly(4-methyl-1-pentene) (PMP) using a dry process. Compared with PP and PE, PMP has a higher melting temperature of about 235 °C. The PMP precursor film produced by a tubular extrusion process (dry process) showed a semicrystalline structure with planar-stacked lamellae. The stacked lamellar morphology and the orientation state of the membranes heavily relied on the extrusion stress and the weight-average molecular weight ($M_w$) of PMP. The evaluation of this type of membranes as battery separators was not presented.

Porous power technologies fabricated PVDF separators using the evaporation-induced phase separation process [41]. Acetone and water were used as the solvent and nonsolvent, respectively. The separator showed a high porosity of about 80%, and the batteries with this porous PVDF separator exhibited reduced internal resistance. However, investigations on the abuse tolerance (i.e., tolerance of short) of this type of separators need to be conducted as PVDF losses its mechanical strength in liquid electrolytes, especially when the temperature is high.

Attempts have been made to improve the battery abuse tolerance through increasing the thermal stability of the separator by using high-temperature polymers (such as polyamide and polyimide). These activities mostly remain in the research stage and the membranes are mainly being prepared using the phase-inversion approach. A paraoriented polyamide porous film comprising of fibrils having a diameter less than 1 μm has been fabricated [42]. The polyamide solution was first cast into a film and then cooled to deposit the polyamide. Next, the film was immersed in an aqueous or alcoholic solution to elute the solvent. The dry porous film exhibited good mechanical properties and a porosity ranging from 38% to 87% with good uniformity. Due to the thermal stability of the aromatic polyamide, its linear thermal expansion coefficient between 200 and 300 °C was about $50\times10^{-6}$/°C. However, its performance in a liquid electrolyte was not discussed.

UBE Industries, Ltd. has developed polyimide separators [43]. The polyimide precursor was a polyamic acid prepared by polymerizing a tetracarboxylic acid and a diamine. A porous precursor film was fabricated through the phase-inversion method by casting the polyamic acid solution, forming a liquid film comprising of a mixture of a solvent and a nonsolvent on a glass substrate, and immersing the cast film into a coagulating solution composed of the solvent and the nonsolvent. The precursor film was then dried and imidized into a polyimide porous film. The resulting polyimide separator showed relatively uniform pore size distribution. Although the membrane had no thermal shutdown ability, it offered excellent thermal stability.

Overcharge protection has also been investigated through the separator design [44–47]. Xiao et al. [44] prepared a composite membrane comprised of *p*-poly-

phenyl (PPP) and polyaniline (PAn) layers. The separator was *p*-doped at high-oxidation potentials into a conductive phase to shunt the current and returns to the de-doped isolating state at normal operating voltages. The PPP/PAn composite separator was evaluated in a Li/$LiMn_2O_4$ cell. When cycled between 3.6 and 4.3 V at 25 mA/g, the composite separator showed behaviors similar to a commercial PP porous membrane. However, upon overcharging, the voltage of the cell with the PP separator rose to 4.8 V in 8 min, while the voltage of the cell containing the composite separator showed a steady plateau at 4.31 V. Chen and Richardson [45] impregnated a PP porous separator with an electrochemically active poly(3-butylthiophene) for overcharge protection. $TiS_2$, Li, and 1 M $LiPF_6$ in PC/EC (1:1 by volume) were used as the cathode, the anode, and the electrolyte, respectively. When charged at a C/10 rate to a limit of 4 V, the discharge capacity of the cell with a regular PP separator degraded rapidly due to the degradation of the cathode. The cell with the poly(3-butylthiophene) impregnated separator was undamaged by overcharging up to ten times the normal capacity, since poly(3-butylthiophene) shunted the excess charge and limited the potential to about 3.2 V. However, at 1 °C rate overcharging, the overcharge protection was not achieved. Feng et al. [46] used an electroactive polytriphenylamine as the separator material. Upon testing Li/$LiFePO_4$ cells, the experimental results demonstrated that the electroactive separator produced a resistive internal short circuit to maintain the cell voltage near 3.75 V at overcharge. However, for this type of separator, the major barriers to practical applications are the battery self-discharge and the effectiveness of the overcharge protection, especially at a charge rate.

*Separator modification* Pristine polyolefin membranes lack sufficient compatibility with the electrodes and carbonate solvents. However, good surface contact between separators and electrodes is critical since a poor interface can cause an uneven current distribution resulting in the formation of Li dendrites and increase the battery internal resistance deteriorating the battery performance.

The modification of membranes has then been conducted to optimize the performance of the separator and the overall battery system. Grafting polymerization can attach functional groups on the membrane surface through covalent bonding so as to change the separator surface polarity permanently. Ko et al. [48] used an electron beam to attach glycidyl methacrylate on the surface of a porous PE separator. They attributed the improved life cycle of the mesocarbon microbeads/$LiCoO_2$ cell to an enhanced electrolyte holding capability and a reduced interfacial resistance. Similarly, Gao et al. [49] grafted methylmethacrylate on polyolefin separators by an electron-beam-induced polymerization; Gineste and Pourcelly [50] modified a PP membrane with acrylic acid (AA) and diethyleneglycol-dimethacrylate by electron beam irradiation; Yao and Ranby [51] developed a continuous process for the modification of polyolefin separators with AA through an ultraviolet irradiation for alkaline batteries; and Urairi et al. [52] treated polyolefin separators with plasma to improve their hydrophilicity for alkaline battery application.

Porous polyolefin membranes have also been laminated with gellable polymer films to improve their compatibility with the electrolyte and electrodes. A separator comprising of a porous polyolefin base and a porous PVDF layer on at least one surface of the base material was proposed [19, 53]. The presence of PVDF provided improved electrolyte retention and bondability to the electrodes. Polyolefin separators have also been laminated with a porous gellable poly(acrylonitrile-methyl methacrylate) layer by dipping the separator in the copolymer solution [12]. The base PE membrane was 25 μm thick, and the coated separator had a total thickness of 30–45 μm. The authors attributed the good capacity retention and rate performance to the strong bonding between the separator and the electrodes. Kim et al. [54] further incorporated ceramic particles into a gellable polymer coating by pasting a 2–3-μm thick layer of gellable polymer containing $SiO_2$ particles on both sides of a base separator membrane. The addition of silica particles showed improved wettability and enabled increased ionic conduction.

## Other types of separators

*Nonwoven mats/webs* Although nonwoven mats/webs have long been used as separators for different batteries, they have very limited applications in Li-ion secondary batteries nowadays. Nonwoven mat separators have certain advantages such as low processing cost, high porosity, and lightweight. In addition, mats with different organic and inorganic fibers can be conveniently fabricated to provide high heat resistance and good mechanical properties. However, nonwoven mat separators typically have a large pore size, so to prevent dendrites from growing through the pores, their thickness must be increased. The recent technology has made the fabrication of nanofiber nonwoven mats feasible. Thin nonwoven separators can thus be produced with nanofibers, which provide the potential for Li-ion battery applications. A nonwoven mat is usually produced through a dry laid process, a wet-laid process, a melt-blown process, or an electrospinning process. These processes allow fiber adhesion by sprayed resin bonding, thermoplastic fiber bonding, fiber self bonding, or mechanical bonding.

The air-laid process is a dry process where individualized staple fibers are air conveyed onto a moving belt to form a mat. A latex binder is applied at the same time to incorporate

the mechanical integrity. The formed mat can also be thermally bonded through a calendaring process.

The wet-laid process can be conducted on a papermaking machine. Fibers are first suspended in water. Paper machines are used to separate water to form a uniform web, which is then bonded and dried to achieve mechanical integrity. Kritzer [55] fabricated a polyester mat using this wet-laid process. Polyester fibers together with binder fibers were suspended in water and randomly laid on a screen belt. The nonwoven mat, formed by drying the fiber suspension, was thermally bonded at 230 °C. The electrochemically and thermally stable nonwoven mat showed an average pore size of 20–30 μm and a porosity of 55–65%. Pinholes were not observed due to the labyrinth-like structure of the nonwoven material, yet, because of the large mean pore size, this nonwoven mat was not used as a separator directly, but as a support layer for battery separators. Ashida and Tsukuda [56] disclosed the fabrication of a nonwoven mat made by blending organic and up to 80 wt.% ceramic fibers through this wet-laid process showing improved heat resistance. Organic fibers such as polyolefin and polyamide fibers were used to improve formability and increase strength. The separator showed good adhesion to the electrodes, displaying no signs of slippage or gaps between the separator and the electrodes, during the fabrication of the battery. Wang et al. [57] prepared a wet-laid nonwoven separator using fibrillated aromatic polyamide fibers observing, thereafter, an improved permeability and electrolyte absorption rate compared with a conventional polyolefin separator. Capillary porometer tests showed the average pore sizes of the two mats prepared were as small as 0.180 and 0.372 μm, respectively. It should be noted that a capillary porometer measures the smallest pore constraints.

Melt-blown mats are formed by extruding molten polymers through a die and then attenuating the resulting filaments with a high-velocity air to fine diameters. This is a promising low-cost process to fabricate thermally stable thin membranes suitable for battery separator applications. The preparation of thin but strong separators made of polyester, polyamide, and polymethylpentene and its copolymers through this process has been suggested [58–60]. Mats consisting of a fibrous sheet of polymethylpentene showed a high-temperature shutdown characteristic, and those consisting of high temperature polymers such as polyester and polyamide exhibited excellent dimensional stability at elevated temperatures.

Electrospinning/electrospraying is another attractive method for preparing nonwoven mats, especially those composed of nanofibers. The electrospinning/electrospraying process is conducted by applying a strong electric field to a polymer solution and collecting a fine-charged jet from a small orifice on a grounded collector. The mat morphology is affected by the solvent evaporation rate, the polymer concentration, the distance from the nozzle tip to the target, the accelerating voltage, etc. The fibers fabricated through this process can be submicron or nanometer sized. Thus, electrospun mats can have much smaller thickness compared with those fabricated by other mat-forming processes. Due to the challenges of designing high-throughput electrojetting processes, investigation continues to be exploratory and no commercial battery separators are currently available. Porous membranes composed of submicron fibers made of polyimide [61], polyacrylonitrile (PAN) [62], and PVDF [63, 64] have been investigated. Bansal et al. [61] prepared a polyether imide nanofiber web through electrospinning. Polyimide and the blends of polyimide and PAN/PVDF-HFP were spun into mats with 65–85% porosity. However, the effect of liquid electrolytes on the properties of these mats was not discussed and their performance in a real battery was not systematically investigated. Cho et al. [62] prepared porous PAN separators using the electrospinning process. The fibers had a homogeneous diameter of 250–380 nm. Compared with the conventional porous separators, PAN nonwoven mats showed better cycling performance and rate capability at room temperature. Kim et al. [63] was able to control the pore size and porosity PVDF-HFP porous membranes by electrospinning the copolymer solutions of distinct polymer concentration. The electrospun polymer separators enabled good ionic conduction at room temperature and a wide electrochemical stability window of up to 4.5 V vs. $Li^+/Li$ when 1 M $LiPF_6$ in EC/DMC/DEC (1/1/1 by weight) was used as the electrolyte.

In another effort, electrospinning was modified into an electroblowing process by simultaneously applying electrical force and an air shearing force [65–69]. An air-blowing system, with flow and temperature control, delivered a high-velocity air around the spinneret along the fiber spinning direction. This process resulted in higher efficiency and yield-combining characteristics of electrospinning and melt-blowing processes [65].

Currently, nonwoven mats are mainly used as a support layer for separators. Patent application WO06123811 disclosed a separator for Li-ion batteries produced by coating a nonwoven mat with porous aromatic polyamide layers on both sides [70]. The poly(ethylene terephthalate) (PET) nonwoven mat with a thickness less than 30 μm was fabricated through the wet-laid process and the polyamide coating was applied through the phase-inversion method. The separators showed high heat resistance, and no shrinkage was observed when tested at 150 °C for 2 h. Lee et al. [71, 72] coated a porous PVDF layer on the surface of a PE nonwoven mat of 20 μm thick. The PVDF coating was applied by casting a solution of PVDF in *N*-methylpyrrolidone on the PE mat and then, by the phase-

inversion method, converted to a 33-μm thick porous structure. The authors reported that these separators displayed sufficient mechanical properties and improved capacity retention in Li-ion cells. Pekala and Khavari [73] passed a ~18-μm thick porous UHMWPE nonwoven mat through a hot PVDF solution bath impregnating the polymer into the mat. The time required to achieve a uniform electrolyte distribution throughout the battery was reduced with this PVDF-coated mat due to increased compatibility with the battery system.

Ceramic coatings have also been applied on nonwoven mats for improved thermal performance. This topic is covered in the following section.

*Composite/ceramic-enhanced separators* As mentioned earlier, to improve the battery abuse tolerance, Li-ion battery separators with high thermal stability are needed, especially for applications in EVs or HEVs. This can be achieved either by using high melting temperature polymers, such as polyamide and polyimide (as described in the previous sections), or by incorporating inorganic fillers into the porous or nonwoven membranes. The latter are called composite or ceramic-enhanced separators. In general, composite separators have excellent wettability by the nonaqueous electrolyte solvents, even when the temperature is low. These separators also show excellent thermal stability, which is critical to ensure satisfactory battery abuse tolerance at high temperatures. In addition, inorganic ceramic particles have relatively high thermal conductivity, thus, dissipating heat at a fast rate. Due to the above-mentioned advantages, composite separators have attracted increasing attention recently. However, although composite separators generally offer high punch strength, their tensile strength is usually lower compared with the plain polymeric separators. Other potential issues related to ceramic-enhanced separators are increased separator weight due to the incorporation of heavy ceramic particles, unknown electrochemical stability of the ceramic and the ceramic binder in the highly oxidizing and reducing environments encountered in Li-ion batteries, and particle shedding due to the insufficient binding.

Composite separators can be produced by binding micron or submicron ceramic particles with polymeric binders. Zhang et al. [74] prepared a freestanding and flexible porous membrane by using $CaCO_3$ particles as the main component and 2–8 wt.% of polytetrafluoroethylene (PTFE) as the binder. The process for producing the membrane involved dispersing 10 μm $CaCO_3$ particles in a PTFE dispersion, casting and hot rolling the dispersion into a flexible membrane with a thickness of 175–190 μm, and drying the membrane at 120 °C under vacuum. However, to reduce the membrane thickness for realistic applications, smaller particles will need to be used. The authors evaluated the membrane with a $CaCO_3$/PTFE weight ratio of 92/8 by soaking it in a liquid electrolyte of 1 M $LiPF_6$ in a mixture of EC and EMC (3:7 by weight). The "effective ionic conductivity" of the electrolyte wetted membrane was 2.4 mS/cm at 20 °C as compared with 8.0 mS/cm for the virgin liquid electrolyte. However, the compatibility of the filler with the battery components, especially the liquid electrolyte, needs to be investigated.

Cho et al. [75] fabricated a ceramic separator by casting PE–PP sheath-core composite fibers (a fiber diameter of 2 μm) with nanosized silica particles using an air-laid process. The formed webs were thermally bonded in an oven. The cell was assembled using $LiCoO_2$ as the cathode, graphite as the anode, and 1 M $LiPF_6$ in EC/DEC (1/1 by volume) as the electrolyte. The composite separator showed improved wettability and better performance than neat polyolefin-based membranes when cycled in the voltage range of 3.0–4.2 V at a C/2 rate. The composite membrane was thermally stable, and its shrinkage at 150 °C was only 3%, as compared with the 37% shrinkage for a conventional PP separator. The authors also claimed that in order to suppress the microshorting caused by the Li dendrite growth, the Gurley number for this type of separators must be higher than 200 s/100 $cm^3$.

Lamination by coating a supporting porous polyolefin or nonwoven structure with a layer of inorganic particles has also been used to fabricate freestanding ceramic-enhanced separators. Shinohara et al. [76] fabricated a heat-resistant membrane by coating a mat or porous film with a dispersion of ceramic particles in a heat-resistant aromatic polymer solution of either a polyamide or a polyimide. The prepared laminate membranes typically showed a porosity of about 45% and a tensile strength of above 45 MPa.

Evonik–Degussa commercialized a ceramic separator by coating an ultrathin PET nonwoven support layer with oxides including alumina, zirconia, and silica, as shown in Fig. 5 [8, 77–79]. Oxide particles were first suspended in an inorganic binder sol that was prepared by hydrolyzing a mixture of tetraethoxysilane, methyltriethoxysilane, and (3-glycidyloxypropyl) trimethoxysilane in the presence of a HCl aqueous solution. The suspension was then coated on a nonwoven PET mat. A composite separator was obtained by drying the coated PET at 200 °C. The obtained separator had a small average pore size of 0.08 μm and a thickness of about 24 μm. For this type of separators, the PET nonwoven of about 20 μm thick provides the tensile strength and flexibility, while the fine ceramic particle coating helps avoid pinholes while providing dendrite penetration resistance and thermal stability.

LG Chem also developed ceramic-enhanced separators [80–83]. The separator was produced by coating a porous substrate (typically a polyolefin porous film) with a porous layer formed by casting a slurry of inorganic particles and a

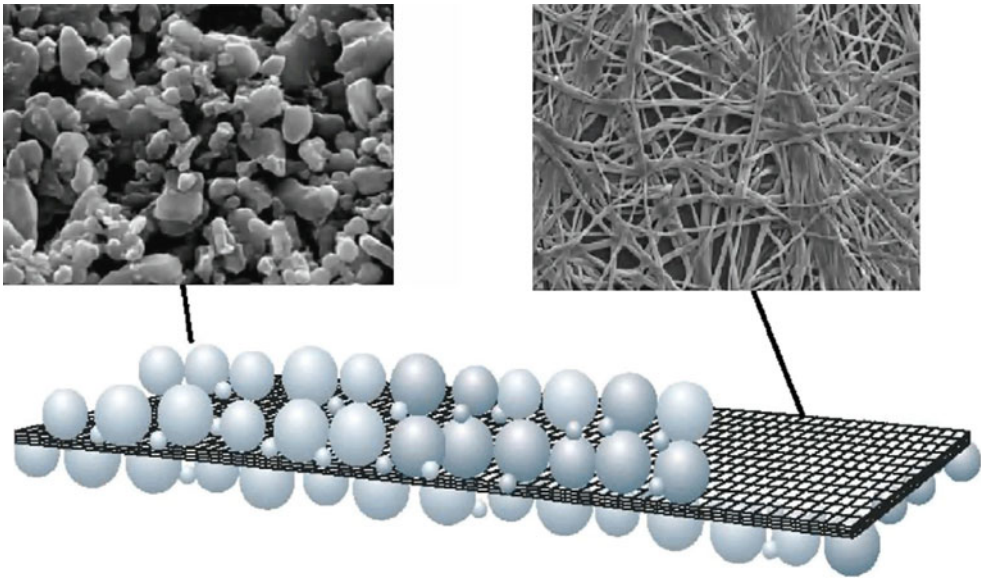

**Fig. 5** Schematic of an Evonik–Degussa ceramic separator [8, 77]

polymeric binder. The membrane with a PE support and a $BaTiO_3$/butylacrylate-acrylic acid copolymer-coating layer showed less than 10% shrinkage at 150 °C for 1 h.

Hitachi Maxell Ltd. has reported the development of a thermally stable separator made by coating a polyolefin porous film with metal oxide flakes [84]. The coated separator exhibited a shrinkage of less than 5% even at 180 °C.

In addition, composite separators have been fabricated simply by adding ceramic particles into the material formulations for making separators using the wet process. Sony Corporation developed a separator composed of HDPE and fine alumina particles [85]. A mixture of PE resin, alumina particles and/or inorganic fibers, and mineral oil was kneaded into a sheet at the melting point of the polyolefin resin. A porous membrane was formed through the extraction of the mineral oils.

Besides the applications in porous separators for liquid electrolyte batteries, ceramic powders have also been used in a gel polymer electrolyte (gel polymer separator). The effects of $SiO_2$ [86], $Al_2O_3$ [87], $TiO_2$ [88], and MgO [89] on the electrochemical properties of gellable-polymer-based electrolytes have been studied. It has been shown that the incorporation of ceramic powder enhances the ionic conductivity, improves the mechanical and thermal stability, and provides high chemical integrity (no liquid leakage) even at elevated temperatures. The improvement has been attributed to the change of the molecular morphologies and physical properties of the polymers due to the addition of the inorganic particles. Abraham et al. [90] prepared a ceramic-PVDF electrolyte separator and Hikmet [91] obtained a porous $Li_{0.35}La_{0.55}TiO_3$-UHMWPE separator. However, they stated that addition of the ceramic particles did not significantly change the conductance.

Composite separator layers have also been coated on an electrode directly to reduce the production cost. Less et al. [92] applied separator coating on an electrode by spraying a dispersion of fumed silica in a PVDF solution. When the silica/PVDF weight ratio was 65/35, the separator coating showed a $N_M$ similar to a commercial polyolefin separator. Kim et al. [93] formed composite separators by a dip-coating approach. The nanoalumina loading in the ceramic-coating layer was up to 94 wt.% with the rest being a PVDF binder. The cell with this separator coating showed enhanced rate performance when compared with a cell with a conventional separator.

## Numerical modeling of Li-ion cells/separators

Since the porous separators have very complex pore structures, a simplified analysis has been employed to evaluate the effect of separators in practice [94, 95]. The following empirical equation (Eq. 6) has been used extensively in mathematical modeling.

$$R_s = \varepsilon^{-\alpha} \cdot R_0 \tag{6}$$

where $R_s$ is the resistance of the separators filled with the liquid electrolyte, $R_0$ is the resistance of the native liquid electrolyte, $\varepsilon$ is the void volume fraction in a separator, and $\alpha$ is the Bruggeman exponent. However, Patel et al. [11] found that only porous membranes with idealized morphologies (spherical or slightly prolate ellipsoids) followed the Bruggeman law with an $\alpha$ of about 1.3. Porous networks based on other particle morphologies resulted in either a significant increase in $\alpha$, or a complete deviation from the power law, mainly due to the increased tortuosity. The models indicated that spherical or slightly prolate ellipsoidal pores should be preferred for batteries where a high-rate performance is required.

Thorat et al. [96] developed an empirical relationship between porosity and the tortuosity of the porous structures. Their results demonstrated that the tortuosity-dependent mass transport resistance in porous separators and electrodes was significantly higher than predicted by the frequently used Bruggeman relationship. Tye [16] investigated the effect of tortuosity on the electrolyte diffusion ingress response of a separator. He showed that separators with identical average tortuosities and porosities could have different unsteady-state behaviors due to the difference in tortuosity distributions. Newman and Srinivasan [97] studied the performance of a natural graphite/$LiPF_6$ in a mixture of EC and DEC/iron phosphate lithium-ion cell. They built a model to optimize the porosity and thickness of the positive electrode, the thickness and porosity of the separator, the electrolyte concentration, and the porosity of the negative electrode. Xiao et al. [98] attempted to evaluate the stress field in a separator during normal battery cycling. The current industrial requirement on the separator tensile property comes from the battery assembly demands. The stress distribution in a separator when the battery is under normal cycling conditions is not well understood. This work has indicated that the stress is affected by the active material properties, electrode geometries, separator wrapping patterns, charging–discharging protocols, etc.

## Future work

In the light of the above discussion, the goals of the future research will be to (1) develop low-cost fabrication processes, (2) discover new materials with high thermal stability, (3) further understand the behavior of separators during the operation of the battery, and (4) extend the functions of the separator in a battery in order to improve the battery performance under all operating conditions expected in the automotive usage. Abuse tolerance and cost are especially important for large-scale applications in HEV/EV and should drive all these research directions.

The modification of commonly used polyolefin microporous separators can lead to improved separator performance. The modification can be achieved by coating and chemical crosslinking. Ceramic separators have shown excellent thermal stability and electrolyte wettability. Increasing numbers of ceramic separators have been commercialized to meet the abuse tolerance and performance requirements for HEV/EV applications. Development of modern processes, from an interdisciplinary approach, may lower the production costs. Nonwoven mats of nanosized fibers have the potential to be used as low-cost separators with good thermal stability and should be developed for battery applications. Numerical modeling should assist the design of separators for improved battery abuse tolerance and performance. Effort in this area is still needed in order to further optimize the separator performance in future battery systems.

## Conclusions

Semicrystalline polyolefin-based microporous separators have dominated the Li-ion separators market. They have small thickness, excellent chemical resistance, and good mechanical properties. However, polyolefin separators generally are not thermally stable. They shrink significantly at 90–120 °C and melt at 150–200 °C depending on the type of the polymers. Ceramic-enhanced composite separators exhibit the advantages of good liquid electrolyte wettability and the ability to prevent thermal runaway conditions in the event of an internal short, which is critical in high-power applications. Although traditional nonwoven separators have a low production cost and exhibit good thermal stability, they have a large thickness, which reduces the energy and power densities of a battery, and a large mean pore size, which increases the risk of internal shorting through dendrite growth. Recent techniques for fabricating nonwoven mats comprised of nanosized fibers augment the feasibility for producing high-performance separators with high tortuosity, high porosity, and good thermal stability. The modification (including ceramic coating, crosslinking, and functionalization) of polyolefin microporous separators and the development of alternative polymers for porous membranes are also the potential directions for improving the performance of separators.

**Acknowledgments** The author would like to thank Ion C. Halalay, Ingrid A. Rousseau, Hamid G. Kia, and Mark W. Verbrugge at General Motors and Jonathon Hitt at Optimal Resources LLC for the valuable discussions.

## References

1. Ehrlich GE (2002) In: Linden D, Reddy TB (eds) Handbook of batteries, 3rd edn. McGraw-Hill, New York
2. Johnson BA, White RE (1998) J Power Sources 70:48–54
3. Djian D, Alloin F, Martinet S, Lignier H, Sanchez JY (2007) J Power Sources 172:416–421
4. Jansen AN, Kahaian AJ, Kepler KD, Nelson PA, Amine K, Dees DW, Vissers DR, Thackeray MM (1999) J Power Sources 81–82:902–905
5. Orsini F, du Pasquier A, Beaudouin B, Tarascon JM, Trentin M, Langenhuizen N, de Beer E, Notten P (1999) J Power Sources 81–82:918–921
6. Liu HK, Wang GX, Guo Z, Wang J, Konstantinov K (2006) J Nanosci Nanotechno 6:1–15
7. Arora P, Zhang Z (2004) Chem Rev 104:4419–4462
8. Zhang SS (2007) J Power Sources 164:351–364
9. Caldwell DL, Poush KA (1984) US Patent 4464238
10. Abraham KM (1993) Electrochim Acta 38:1233–1248

11. Patel KK, Paulsen JM, Desilvestro J (2003) J Power Sources 122:144–152
12. Jeong YB, Kim DW (2004) J Power Sources 128:256–262
13. Venugopal G, Moore J, Howard J, Pendalwar S (1999) J Power Sources 77:34–41
14. Piatkiewicz W, Rosinski S, Lewinska D, Bukowski J, Judycki W (1999) J Membr Sci 153:1–102
15. Jena A, Gupta K (2002) Fluid Part Sep J 4:227–241
16. Tye FL (1983) J Power Sources 9:89–100
17. Liu SJ, Maslivah JH (1996) In: Schramm LL (ed) Suspensions: fundamentals and applications in the petroleum industry. American Chemical Society, Washington
18. Kim LU, Kim CK (2006) J Polym Sci Polym Phys 44:2025–2034
19. Ma JC, Megahed ES, Stachoviak TJ, Craanen SA, Schneider DA, Nestler JP (2002) US Patent 6444356
20. Yoneda H, Nishimura Y, Doi Y, Fukuda M, Kohno M (2010) Polym J 42:425–437
21. Weighall MJ (1991) J Power Sources 34:257–268
22. Strathmann H, Kock K (1977) Desalination 21:241–255
23. Yilmaz L, McHugh AJ (1986) J Membr Sci 28:287–310
24. Reuvers AJ, van der Berg JWA, Smolders CA (1987) J Membr Sci 34:45–65
25. Reuvers AJ, Smolders CA (1987) J Membr Sci 34:67–86
26. Radovanovic P, Thiel SW, Hwang ST (1992) J Membr Sci 65:213–229
27. Wienk IM, Boom RM, Beerlage MAM, Bulte AMW, Smolders CA, Strathmann H (1996) J Membr Sci 113:361–371
28. Bottino A, Camera-Roda G, Capannelli G, Munari S (1991) J Membr Sci 57:1–20
29. Zhang SS, Xu K, Foster DL, Ervin MH, Jow TR (2004) J Power Sources 125:114–118
30. Andrieu X, Laurence J (1998) US Patent 5811205
31. Dupasquier A, Tarascon JM (2003) US Patent 6537334
32. Dupasquier A, Warren PC, Culver D, Gozdz AS, Amatucci GG, Tarascon JM (2000) Solid State Ionics 135:249–257
33. Li ZH, Zhang P, Zhang HP, Wu YP, Zhou XD (2008) Electrochem Commun 10:791–794
34. Lundquist JT, Lundsager B, Palmer NI, Troffkin HJ, Howard J (1987) US Patent 4650730
35. Yu WC (1997) US Patent 5691077
36. Higuchi H, Matsushita K, Ezoe M, Shinomura T (1995) US Patent 5385777
37. Ihm DW, Noh JG, Kim JY (2002) J Power Sources 109:388–393
38. Noumi S, Yamamura Y, Nakayama S (2010) US Patent 7704597
39. Yamamoto K, Fujita S, Uetani Y, Noumi S, Emori H, Yamamura Y (2003) US Patent 6559195
40. Johnson MB, Wilkes GL (2002) J Appl Polym Sci 83:2095–2113
41. Beard KW (2006) US patent application 20060081530
42. Takahashi T, Tateno T (1999) US Patent 5856426
43. Ohya S, Fujii Y, Yao S, Asano Y, Nakayama K, Fukunaga K (2003) US Patent 6565962
44. Xiao LF, Ai XP, Cao Y, Wang YD, Yang HX (2005) Electrochem Commun 7:589–592
45. Chen G, Richardson TS (2004) Electrochem Solid-State 7:A23–A26
46. Feng JK, Ai XP, Cao YL, Yang HX (2006) J Power Sources 161:545–549
47. Thomas-Alyea KE, Newman J, Chen G, Richardson TJ (2004) J Electrochem Soc 151:A509–A521
48. Ko JM, Min BG, Kim DW, Ryu KS, Kim KM, Lee YG, Chang SH (2004) Electrochim Acta 50:367–370
49. Gao K, Hu GX, Yi TF, Dai CS (2006) Electrochim Acta 52:443–449
50. Gineste JL, Pourcelly G (1995) J Membr Sci 107:155–164
51. Yao ZP, Ranby B (1990) J Appl Polym Sci 41:1469–1478
52. Urairi M, Tachibana T, Matsumoto K, Shinomura T, Iida H, Kawamura K, Yano S, Ishida O (1996) US Patent 5558682
53. Sugiyama M, Totsuka H, Mitani S, Takahata M (2007) US Patent 7311994
54. Kim JY, Kim SK, Lee SJ, Lee SY, Lee HM, Ahn S (2004) Electrochim Acta 50:363–366
55. Kritzer P (2006) J Power Sources 161:1335–1340
56. Ashida T, Tsukuda T (2001) US Patent 6200706
57. Wang Y, Zhan H, Hu J, Liang Y, Zeng S (2009) J Power Sources 189:616–619
58. Kamei T, Yamazaki M (2004) US Patent 6730439
59. Suzuki H, Sudo Y (2003) JP-A-2003-142064
60. Sudou Y, Suzuki H, Nagami S, Ikuta K, Yamamoto T, Okijima S, Suzuki S, Ueshima H (2007) US Patent 7183020
61. Bansal D, Meyer B, Salomon M (2008) J Power Sources 178:848–851
62. Cho TH, Sakai T, Tanase S, Kimura K, Kondo Y, Tarao T, Tanaki M (2007) Electrochem Solid-State 10:A159–A162
63. Kim JR, Choi SW, Jo SM, Lee WS, Kim BC (2005) J Electrochem Soc 152:A295–A300
64. Lee SW, Choi SW, Jo SM, Chin BD, Kim DY, Lee KY (2006) J Power Sources 163:41–46
65. Chu B, Hsaio BS, Fang D (2006) US Patent application 2006049542
66. Um IC, Fang D, Hsiao BS, Okamoto A, Chu B (2004) Biomacromolecules 5:1428–1436
67. Armantrout JE, Bryner MA, Davis MC, Kim YM (2006) US Patent application 2006012084
68. Kim YM, Sung YB, Jang RS, Ahn KR (2009) US Patent 7618579
69. Peng M, Sun Q, Ma Q, Li P (2008) Microporous Mesoporous Mater 115:562–567
70. Hiroki S, Satoshi N, Hiroyuki H, Takahiro D (2006) Patent application WO 06123811
71. Lee YM, Kim JW, Choi NS, Lee JA, Seol WH, Park JK (2005) J Power Sources 139:235–241
72. Lee YM, Choi NS, Lee JA, Seol WH, Cho KY, Jung HY, Kim JW, Park JK (2005) J Power Sources 146:431–435
73. Pekala RW, Khavari M (2003) US Patent 6586138
74. Zhang SS, Xu K, Jow TR (2005) J Power Sources 140:361–364
75. Cho TH, Tanaka M, Onishi H, Kondo Y, Nakamura T, Yamazaki H, Tanase S, Sakai T (2008) J Electrochem Soc 155:A699–A703
76. Shinohara Y, Tsujimoto Y, Nakano T (1999) US Patent 6447958
77. Augustin S, Hennige VD, Horpel G, Hying C (2002) Desalination 146:23–28
78. Henninge V, Hying C, Horpel G (2010) US Patent 7807286
79. Hennige V, Hying C, Horpel G, Novak P, Vetter J (2010) US Patent 7709140
80. Kim SK, Sohn JY, Park JH, Jang HM, Shin BJ, Lee SY, Hong JH (2010) US Patent 7709152
81. Park JH, Lee SY, Hong JH, Nam MJ, Yoo JA, Kim SS, Han CH (2010) US Patent 7695870
82. Seo DJ, Kim K, Hong JH, Sohn JY, Lee SY, Ahn SH (2007) US Patent application 20070122716
83. Lee SY, Seo DJ, Sohn JY, Kim SK, Hong JH, Kim YS Jang HM (2009) US Patent 7638241
84. Katayama H, Kojima E, Aoyama S, Sato Y (2008) Patent application WO08029922
85. Tomi H, Sato E, Murayama S, Itou F, Imoto H (2006) Japan Patent JP3831017
86. Lee KH, Lee YG, Park JK, Seung DY (2000) Solid State Ionics 133:257–263
87. Appetecchi GB, Romagnoli P, Scrosati B (2001) Electrochem Commun 3:281–284
88. Chung SH, Wang Y, Persi L, Croce F, Greenbaum SG, Scrosati B, Plichta E (2001) J Power Sources 97–98:644–648
89. Kumar B, Scanlon L, Marsh R, Mason R, Higgins R, Baldwin R (2001) Electrochim Acta 46:1515–1521

90. Abraham KM, Koch VR, Blakley TJ (2000) J Electrochem Soc 147:1251–1256
91. Hikmet RAM (2001) J Power Sources 92:212–220
92. Less GB, Knapp A, Babinec SJ (2009) US Patent application 20090155678
93. Kim M, Nho YC, Park JH (2010) J Solid State Electrochem 14:769–773
94. Doyle M, Newman J, Gozdz AS, Schmutz CN, Tarascon JM (1996) J Electrochem Soc 143:1890–1903
95. MacMullin RB, Muccini GA (1956) AICHE J 2:393–403
96. Thorat IV, Stephenson DE, Zacharias NA, Zaghib K, Harb JN, Wheeler DR (2009) J Power Sources 188:592–600
97. Srinivasan V, Newman J (2004) J Electrochem Soc 151:A1530–A1538
98. Xiao X, Wu W, Huang X (2010) J Power Sources 195:7649–7660